Composites Part B 192 (2020) 108005

Contents lists available at ScienceDirect

Composites Part B

journal homepage: www.elsevier.com/locate/compositesb

# Synthesis of degradable hyperbranched epoxy resins with high tensile, elongation, modulus and low-temperature resistance

Xu Ma [a], Wenqiang Guo [a], Zejun Xu [a], Sufang Chen [b], Juan Cheng [a], Junheng Zhang [a], Menghe Miao [c], Daohong Zhang [a,*]

[a] Key Laboratory of Catalysis and Energy Materials Chemistry of Ministry of Education & Hubei Key Laboratory of Catalysis and Materials Science, Hubei R&D Center of Hyperbranched Polymers Synthesis and Applications, South-Central University for Nationalities, Wuhan, 430074, China
[b] Key Laboratory for Green Chemical Process of Ministry of Education, Hubei Key Laboratory of Novel Reactor and Green Chemical Technology, School of Chemical Engineering and Pharmacy, Wuhan Institute of Technology, Wuhan, Hubei, 430205, PR China
[c] CSIRO Manufacturing, 75 Pigdons Road, Waurn Ponds, Victoria, 3216, Australia

ARTICLE INFO

*Keywords:*
Hyperbranched polymers
Epoxy resins
Degradation
Mechanical performance
Low-temperature resistance

ABSTRACT

Hyperbranched epoxy resins (HERs) have attracted much interest due to improving homogeneously the ductility and strength of popular diglycidyl ether of bisphenol-A (DGEBA), but the preparation of HERs/DGEBA composites with low-temperature resistance and rapid degradation is still a challenge in the sustainable development of thermoset field. Here we represent self-curable hyperbranched epoxy resins (DSEHP-n, n = 3, 5, 7, 11) to modify DGEBA. DSEHP-n not only increases simultaneously the tensile strength, flexural strength, impact strength, modulus, and elongation by 64.8%, 38.1%, 93.7%, 70.4%, and 50%, respectively, and but also improve remarkably the low-temperature resistance and degradation degree. The improvement of mechanical properties is caused by the combined effect of crosslinking density, free volume, intermolecular cavity, hyperbranched topological structure, and good compatibility, the account of an in-situ reinforcing and toughening mechanism which substantiated by dynamic light scattering (DLS), SEM, DMA, and free volume analysis. The detailed analysis of degradation products from GC-MS spectra showed that the degradation of the composites was attributed to the cleavage of the C–N and ester bonds. This paper will bring a novel method to prepare highly-efficient degradable thermosets and composites.

## 1. Introduction

Thermoset resins play a vital role in our lives owing to their excellent thermal and mechanical properties [1], including good adhesion [2], corrosion resistance [3], high chemical stability and excellent dielectric property, and they are widely used [4,5] in electronic appliances, automobiles, and coatings, adhesives, fiber-reinforced polymer composites.

Hyperbranched epoxy resins (HERs) [6] have attracted extensive attention in academia and industry due to its high crosslinking ability and hole containing topological structure. On the other hand, their strong crosslinks result in their inability to reprocessing and reshaping by heat or solvent [7,8], and causes extreme difficulties in degradation and recycling [9] and harm to the environment [10,11].

Currently, thermoset wastes are mostly disposed by landfill or incineration, taking up land resources and causing environmental pollution. Several methods for decomposing cured thermoset epoxy resins (EPs) are being developed, including mechanical grinding [12], pyrolysis [13], biodegradation [14] and supercritical fluid process [15]. Mechanical grinding only recycles and reuses the cheap epoxy resins powder. Pyrolysis not only consumes a large amount of energy and is not environmentally friendly. Biodegradation takes a long time and the degraded products are difficult to reutilize. Supercritical fluid process speeds up the degradation of carbon fiber/epoxy composites, but supercritical fluids have a physical etching effect on the carbon fibers [16].

The natural fibers [17,18] may be recycled in cured epoxy resins/natural fibers composites. Another recycling approach is designing renewable or recyclable epoxy resins with thermally cleavable bonds such as ester [19,20], dynamic acetal [21], disulfide [22], imine [23] and hexahydro-s-triazine (HT) structures [24]. To date, several types of degradable epoxy resins carrying these cleavable bonds have been reported. For example, Ma et al. [25] synthesized a disulfide-bonded

* Corresponding author.
*E-mail address:* zhangdh27@163.com (D. Zhang).

https://doi.org/10.1016/j.compositesb.2020.108005
Received 27 February 2020; Received in revised form 20 March 2020; Accepted 23 March 2020
Available online 25 March 2020

epoxy resin (MDS-EPO) due to the presence of a dynamic reversible disulfide bond. Although MDS-EPO can be degraded, it has low strength and can only be used in the field of soft materials. In addition, PDMS/CNTs nanocomposites with high tensile strength and toughness, which are degradable, processable and self-healing, have been developed [26]. By adding trifluoroacetic acid, o-ethylhydroxylamine and benzaldehyde, the degradation of the elastomer can be effectively controlled, but mechanical strength is relatively poor. Yuan et al. [27] have designed new thermosetting resins of poly (hexahydrotriazine) (PHT) via the addition and condensation reactions between aromatic diamines and formaldehyde. It can be degraded under tetrahydrofuran (THF) with HCl solution at room temperature, but it takes a long time.

In strong acid solutions, Hexahydro-s-triazine (HT) will decompose into amine and formaldehyde [10,11]. HERs without HT bonds have poor mechanical properties owing to the poor stability of their thermally cleavable bonds [28]. On the other hand, thermosets containing HT bonds exhibit good degradation in certain conditions, which is strong acid, high modulus, and temperature [10]. García et al. [7] and Yuan et al. [27] synthesized an HT-containing thermoset by condensation between amine and formaldehyde. They used 1-methyl-2-pyrrolidinone as a solvent to accelerate the synthesis of PHT. NMP is toxic and difficult to remove, severely limiting its scope of application. Kaminker et al. [29] designed crosslinked hexahydrotriazine cores using a solvent-free approach, and the crosslinked structure could slowly degrade in 1 mol/L HCl at 20 °C over 20 h. A curing agent (4,4′,4″-(1,3,5-Hexahydro-s-triazine-1,3,5triyl) tris(*N*-(2-aminoethyl) benzamide), HT-A) containing three amino groups was successfully prepared [30]. Compared with 4, 4′-diaminodiphenylmethane cured epoxy resin, HT-A cured epoxy resin has better mechanical and thermal properties.

The above review shows that HERs with HT bonds have excellent mechanical properties and can degrade in relatively mild conditions, and HERs have been used to improve the degradation of DGEBA after curing with limited success. We have prepared degradable hyperbranched epoxy resins [11] (HER-$HT_n$) containing HT bonds by a slow condensation, which showed highly-efficient degradability. However, highly-efficient preparation of degradable HERs and their composites with simultaneous high strength, elongation, modulus, and low-temperature resistance is still a great challenge in the sustainable development of thermosets, as well as highly efficient degradation degree. Inspired by our previous work [11,24], we prepared self-curing and degradable hyperbranched epoxy resins (DSEHP-n, n = 3, 5, 7, 11) through a high efficiency thiol-isocyanate click reaction. When DSEHP-n is added, the degradation and mechanical properties of DGEBA can be improved, showing high-performance DSEHP-n/DGEBA composites with excellent mechanical strength, elongation, modulus, and low-temperature resistance. The degradation mechanism of DSEHP-n/DGEBA after curing blends has been discussed.

## 2. Experimental

### 2.1. Materials

Formaldehyde aqueous solution (37%), ethanol, methylene chloride, chloroform, and nitric acid were supplied by Tianjin Chemical Reagent Co., Ltd. 2-Aminothiophenol (ATP), toluene-2,4-diisocyanate (TDI), triethylamine, $H_2O_2$ and DMF (Meryer Chemical Technology Co., Ltd.). Diglycidyl ether of bisphenol A (DGEBA) was obtained by Yueyang Baling Petrochemical Co., Ltd. The curing agent DETA-AN is prepared from acrylonitrile (AN) and diethylenetriamine (DETA).

### 2.2. Synthesize and property of DSEHP-n

The degradable of DSEHP-n (n = 3, 5, 7 and 11) were prepared by a thiol-isocyanate click reaction and an addition reaction according to Scheme 1. The IHP-n were prepared by a thiol-isocyanate reaction between TDI and HT-BM with various ratio, and IHP-n (n = 3, 5, 7, 11) were obtained by the molar ratios of TDI and HT-BM of 3:1, 7:3, 11:5 and 19:9, respectively, and the detailed process is similar to our previous paper [24].

The FT-IR spectra of DSEHP-n ($cm^{-1}$): 1710 (C═O), 1680 (NH–C═O), 910 (epoxy group). $^1H$ NMR (400 MHz, $CDCl_3$, ppm) spectra of DSEHP-n: 6.54–8.12 (2H, s, $–CH_2$-), 4.92(2H, s, $CH_2$ of s-triazine), 2.01 (2H, s, $CH_2$ of epoxy group), 3.64 (H, m, CH of epoxy group), 4.58 (2H, s, $CH_2$ adhered to the epoxy group). 1.21 (3H, s, $–CH_3$ attached to the benzene ring), 9.03 (H, s, CH of amide group). The degrees of branching (DBs) of DSEHP-n (n = 3, 5, 7 and 11) are 0.53, 0.40, 0.52 and 0.32 and the molecular weights from MALDI-TOF mass are about 1100, 2500, 4500 and 7000 g/mol and the epoxy equivalent weights are about 370, 500, 650 and 650 g/mol, respectively.

### 2.3. Obtaining of DSEHP-n/DGEBA composites

The chemical structure of DSEHP-5, DGEBA, curing agent and the crosslinked structure are shown in Scheme S1 and Scheme S2. The DSEHP-n/DGEBA blends with stoichiometric curing agent (DETA-AN) were cured at room temperature for 12 h and then at high temperature (80 °C) for 6 h in a silicone rubber mold, and finally cooled to room temperature. After that, the cured DSEHP-5/DGEBA blends was ground into fine powder for studying degradation behavior. The curing temperature (80 °C) of DSEHP-5/DGEBA composite is lower than the self-curing temperature [24] (110 °C−190 °C) of DSEHP-5 to restrain $CO_2$ produced during self-curing and to obtain high-performance blends.

## 3. Results and discussion

### 3.1. Rheological behavior of DSEHP-n/DGEBA composites

The key factors influencing on rheological and processing property of epoxy resins blends include viscosity, shear rate, time and temperature, and their relationships about two typical 12 wt% DSEHP-n/DGEBA and DSEHP-5/DGEBA composites have been shown in Fig. 1. With an increase in the time, the viscosities of all DSEHP-n/DGEBA blends changed a little in Fig. 1a–b. However, increasing the DSEHP-n content from 0 to 15 wt% increases the viscosity of blends in Fig. 1a, is attributable to the fact that polar DSEHP-n with high molecular weight increases the entanglement among molecular chains [31], and the reason also supports the change from Fig. 1b along with the rise of molecular weight. The viscosity of composites decreases first sharply and then remains with the increase in temperature in Fig. 1c–d. As temperature rises, the intermolecular distance becomes larger and supplies more spaces to accommodate the motion of molecular or segments [32] between one place and one vacant hole, resulting in the decrease of the entanglement density [33] and intermolecular interactions [32]. Fig. 1e–f shows a shear thinning behavior that the shear viscosity decreases slowly along with raising the shear rate from 20 to 200 $s^{-1}$, suggesting a non-Newtonian rheological behavior of all DSEHP-n/DGEBA composites.

As the frequency increases, the storage modulus (G′) and loss modulus (G″) [34] of all samples monotonically raise, and the G′ is less than G″ in the same sample over the entire frequency in Fig. 2. Increasing DSEHP-5 content from 0 to 15 wt% in DSEHP-5/DGEBA blends, the G' and G" increased by 102.52% and 55.97% at a frequency of 100 rad/s, respectively. Similar results were observed by raising the molecular weight of DSEHP-n. The activation energies of composites can be estimated by the rheological model process [35] and the following equation (1).

$$\eta_0 = \eta(T)\exp\left(\frac{E_a}{RT}\right) \quad (1)$$

where $\eta_0$ is zero shear viscosity at temperature $T$, and $\eta(T)$ is shear viscosity in different temperature, and $Ea$ is apparent activation energy

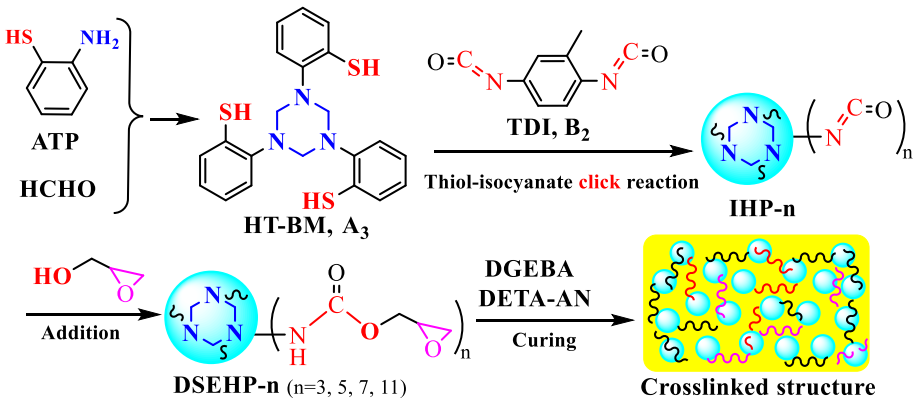


**Scheme 1.** Synthesis and curing process of DSEHP-n.

(kJ/mol), and the value *R* is 8.314 J•mol$^{-1}$/K and *T* is the temperature in Kelvin. The apparent activation energies of 3 wt% DSEHP-5/DGEBA, 6 wt% DSEHP-5/DGEBA, 9 wt% DSEHP-5/DGEBA, 12 wt% DSEHP-5/DGEBA and 15 wt% DSEHP-5/DGEBA composites are 69.89, 71.19, 73.39, 75.09, and 79.15 kJ/mol, respectively, and all which is higher than that of DGEBA (69.63 kJ/mol). Apparent activation energy is expressed as the difficulty of moving a molecule or segments from one location to another, further supporting a conclusion that the composites with a high activation energy results in a high viscosity in Fig. 1.

The average particle size and particle spread of hyperbranched epoxy and DGEBA blends could be obtained availably from dynamic light scattering (DLS) [34,36]. Here, the average particle size and spread of the DSEHP-n/DGEBA blends are seen in Fig. 3. The polar DSEHP-n with high molecular weight increases molecular chains entanglement [31] and strong intermolecular interaction, leading that the average particle size of DSEHP-5/DGEBA blends also increased from 648.48 nm (DGEBA) to 685 nm, 766 nm, 859 nm, 960 nm, and 1077 nm, respectively, with the increasing content of DSEHP-5 from 0 to 15 wt%. This is consistent with the increase in viscosity of DSEHP-5/DGEBA composites with different content of DSEHP-5.

### 3.2. Degradation behavior of DSEHP-n/DGEBA composites

The critical factors influencing the degradation degree of thermoset materials contain the time, temperature, content, and property of materials. Our team has previously studied the degradation of hyperbranched epoxy [13,26], hyperbranched epoxy and DGEBA blends [37,38]. Based on this, the degradation performance of DSEHP-n/DGEBA blends was studied in detail. Taking DSEHP-5/DGEBA as an example to study the degradation mechanism, the reason is that the structure of DSEHP-5 is similar to DSEHP-3, DSEHP-7, and DSEHP-11, and the mechanical properties of DSEHP-5/DGEBA blend are the best. In the previous study, we studied the degradation performance of DSEHP-n self-cured films and obtained the best degradation conditions [24]. So, we firstly put 0.25 g cured 12 wt% DSEHP-5/DGEBA powder into solution with 7.5 g $H_2O_2$, $HNO_3$/DMF (7.5g, 1.0 mol/L) and researched the effect of degradation time on degradation degree under 90 °C, the degradation results are shown in Fig. 4a. With the rise of degradation time, the degradation degree of the blend increased little by little. When the degradation time reaches 6 h, the degradation degree of DSEHP-5/DGEBA is about 99.9%. Prolonging the reaction time can improve the degradation degree of the blend, increasing the reaction temperature can accelerate the degradation reaction, too [39]. It can be seen from Fig. 4b that while the degradation temperature raises from 50 °C to 90 °C, the degradation degree of composite increases from 30.8% to 99.9% under the same other degradation conditions. In addition, with the increase of DSEHP-5 content, the degradation degree of the composite increased gradually. When the content of DSEHP-5 was 12 wt%, the degradation degree reached 99.9% in Fig. 4c. The contents of both ester group and hexahydro-s-triazine structure in blends increase with the rise of the DSEHP-5 content, leading to an increase in degradation degree [24,38]. Due to the similar chemical structure of 12 wt% DSEHP-3/DGEBA, 12 wt% DSEHP-7/DGEBA and 12 wt% DSEHP-11/DGEBA, the degradation degree of them is about 99.9% under the same degradation condition.

GC-MS test was performed on the treated degradation solution, as shown in Fig. S1, and accordingly, the degradation compositions and chemical structures are obtained and shown in Table S1. The supposed degradation mechanism of composites is shown in Scheme 2. The purpose of DMF is to dissolve the degraded small molecules, while $H_2O_2$ is to decompose the cross-linking structure into segments [19,37,40]. The formation of products ***(2)***, ***(5)*** and ***(6)*** are because of the degradation of DGEBA after curing chains [38,40]. The degradation products ***(1)***, ***(3)***, ***(4)***, ***(7)***, and ***(8)*** are formed after the C–N fracture of the curing agent chains [11]. Since the acidic solution contains many protons, a relatively stable five-membered ring structure ***(1)*** could be produced, and compounds ***(9)*** and ***(10)*** also could be obtained. At the same time, the nitro group in the products ***(11)*** resulted from oxidation of amino via the strong oxidation of $H_2O_2$ [41].

### 3.3. Mechanical performance of DSEHP-n/DGEBA composites

The influences of DSEHP-n content and molecular mass on the mechanical performance of DSEHP-n/DGEBA blends after curing are shown in Fig. 5.

The mechanical properties of all blends increase first and then decrease with the addition of DSEHP-n. It is obvious that DSEHP-5 has a greater positive influence on the mechanical strengths of the blend than the other three hyperbranched epoxy resins. Specifically, the maximum tensile strengths of 12 wt% DSEHP-3/DGEBA, 12 wt% DSEHP-5/DGEBA, 12 wt% DSEHP-7/DGEBA and 12 wt% DSEHP-11/DGEBA are 96.9 MPa, 104.5 MPa, 100.2 MPa, and 98.1 MPa, respectively, and all of which are increased by 52.8%, 64.8%, 58%, and 54.7% higher than 63.4 MPa of DGEBA after curing in Fig. 5a. The tensile modulus of 12 wt % DSEHP-5/DGEBA is 5677.03 MPa, which is increased by 86.43% higher than the DGEBA after curing (3045.20 MPa).The flexural strengths of 12 wt% DSEHP-3/DGEBA, 12 wt% DSEHP-5/DGEBA, 12 wt % DSEHP-7/DGEBA and 12 wt% DSEHP-11/DGEBA are 124.7 MPa, 138.8 MPa, 134.9 MPa, and 128.1 MPa, respectively, increased by 24.1%, 38.1%, 34.2%, and 27.4% higher than that (100.5 MPa) of the DGEBA after curing in Fig. 5b. The flexural modulus of 12 wt% DSEHP-5/DGEBA is 3811.43 MPa, which is increased by 64.63% higher than the cured DGEBA (2315.16 MPa). The stress-strain curves in Fig. 5c show that elongation (4.68%) of cured 12 wt% DSEHP-5/DGEBA composites is increased by about 50%, compared with that of cured DGEBA (2.35%). In contrast with impact strength (12.6 kJ/m$^2$) of DGEBA after

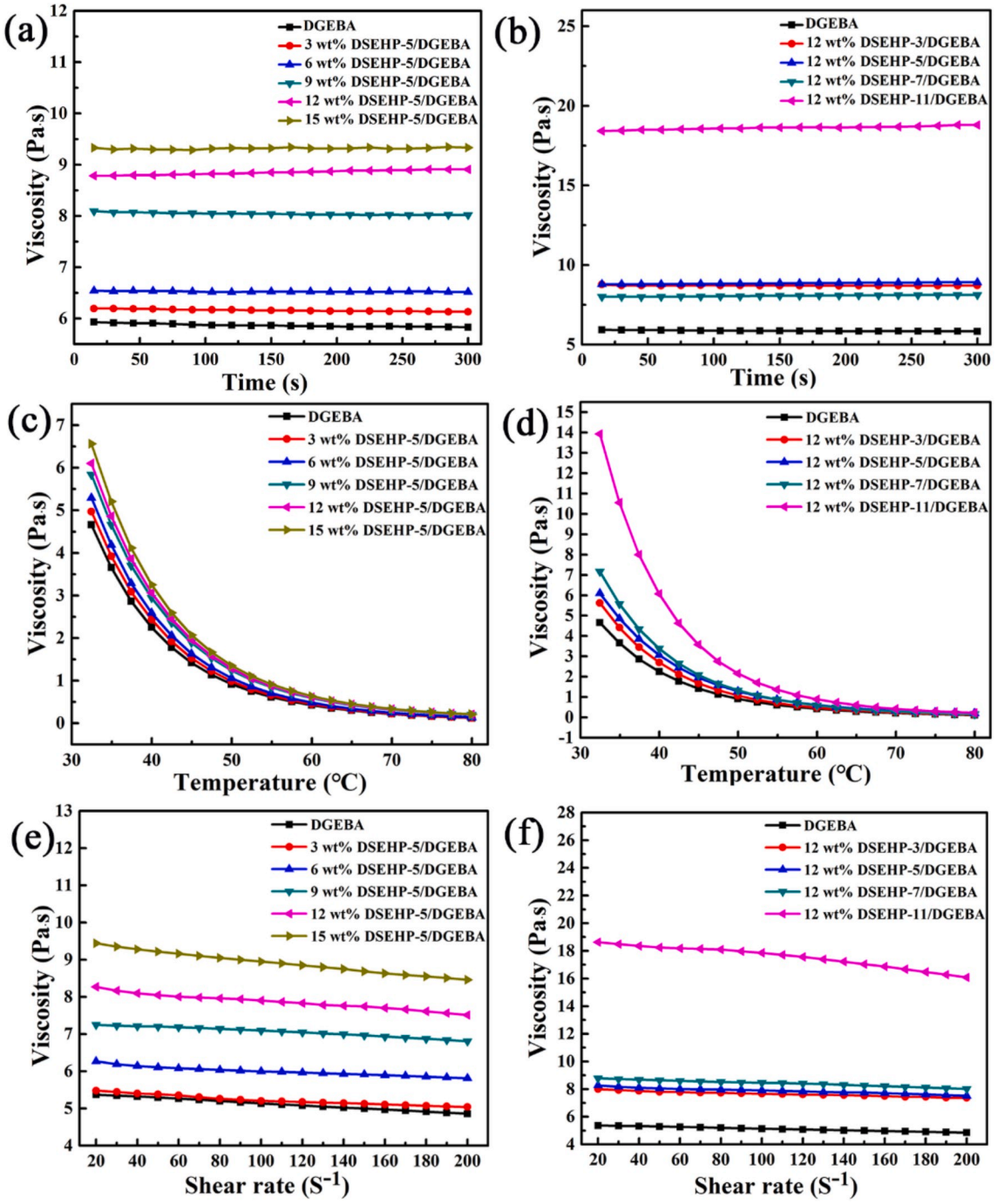


**Fig. 1.** Effects of time (a–b), temperature (c–d), shear rate (e–f) on viscosity of DGEBA and DSEHP-n/DGEBA blends.

curing, the impact strengths of cured 12 wt% DSEHP-3/DGEBA, 12 wt% DSEHP-5/DGEBA, 12 wt% DSEHP-7/DGEBA and 12 wt% DSEHP-11/DGEBA composites improved by 51.6%, 93.7%, 69% and 63.5% in Fig. 5d, respectively.

DSEHP-n can improve the mechanical properties of DGEBA because of the combination [42] of crosslinking density and intermolecular cavities or hyperbranched topological structure. In the wake of the increase of DSEHP-n content, the crosslink density and intermolecular cavities in DSEHP-n/DGEBA also raise. The intramolecular cavity (non-crosslinkable structure in the core of hyperbranched polymers) has a positive influence on impact strength and has a negative influence on stretching and curving strengths, and but the crosslink density has a reverse influence. And the hyperbranched topological structure can absorb impact energy, deform and transfer load, resulting in high elongation [43].

The scanning electron micrographs (SEM) has further investigated the mechanism of impact fracture of the DSEHP-n/DGEBA composites after curing, and their SEM micrographs of the fractured surface after impacting are shown in Fig. 6. The impact profile of cured DGEBA is smooth and without any filaments, being indicative of brittle fracture in Fig. 6a. Many filaments or short fibers are observed on the rough surface of cured DSEHP-n/DGEBA composites in Fig. 6b-i, indicating high toughness or ductile property. And the density and length of the fibers or filaments of cured 12 wt% DSEHP-5/DGEBA composites are much higher than other composites, suggesting the highest toughness, which is consistent with the impact strength in Fig. 6d. On the one hand, impact

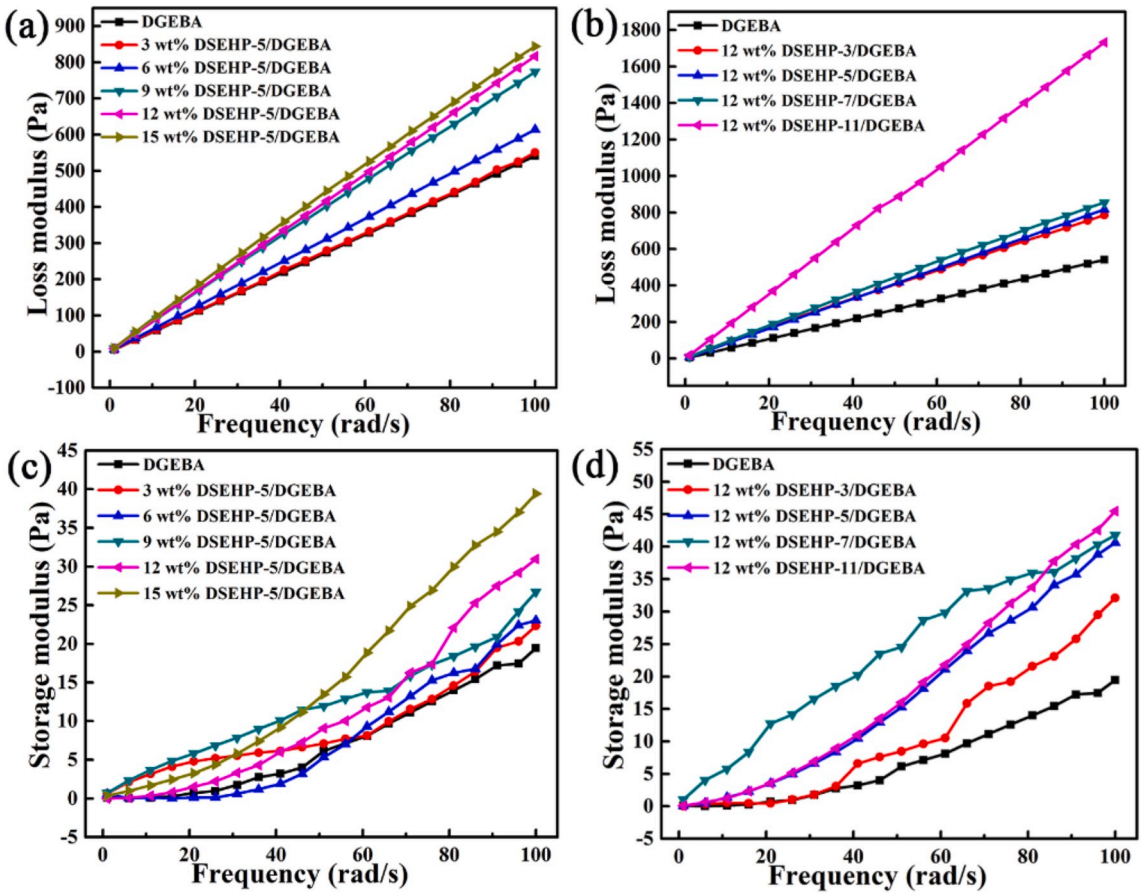


**Fig. 2.** The relationship between frequency and modulus (a, b. loss modulus, c, d. storage modulus) of DGEBA and DSEHP-n/DGEBA blends.

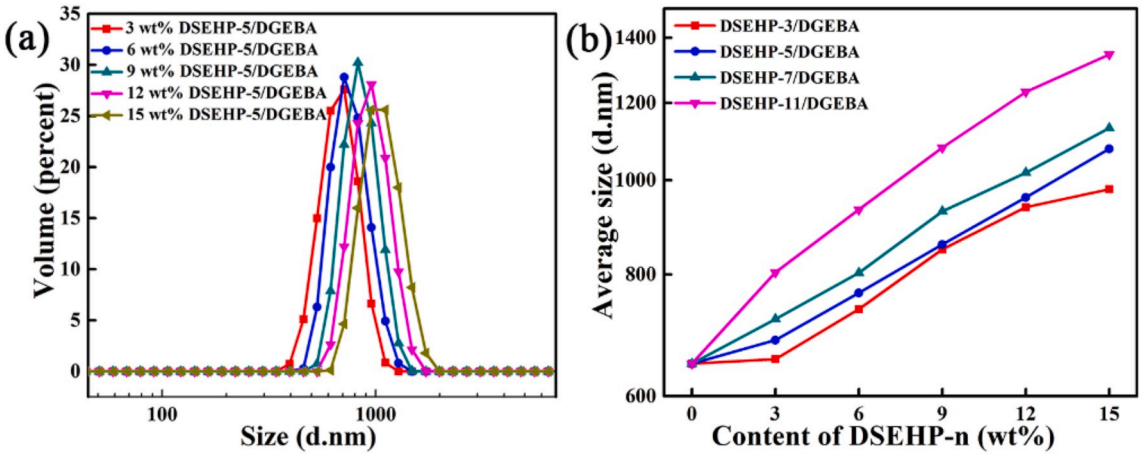


**Fig. 3.** The particle size spread of DSEHP-n/DGEBA blends with (a. various content, and b. molecular weight).

energy can be absorbed by the intermolecular space generated by DSEHP-n through shear deformation [44], improving on toughness. On the other hand, the rigid ring, such as the hexahydro-triazine structure is uniformly dispersed in the DGEBA, and crosslink density takes positive action on strength. Therefore, as DSEHP-n content and molecular weight in DSEHP-n/DGEBA blends raise, the length and thickness of the filaments in the impact cross-section increased in the beginning and then became lower.

The dynamic mechanical properties of the cured DSEHP-5/DGEBA blends with different DSEHP-5 contents were examined and seen in Fig. 7. The storage modulus (É ) represents the stiffness of a viscoelastic material [45]. As can be seen from Fig. 7a, the modulus of DSEHP-5/DGEBA blends after curing were raised, and the reduced with the content of DSEHP-5 increasing, and the maximum appears at 12 wt% DSEHP-5. At room temperature (20 °C), the storage modulus of 6 wt% DSEHP-5/DGEBA, 12 wt% DSEHP-5/DGEBA and 15 wt% DSEHP-5/DGEBA are 1.807 GPa, 2.442 GPa, 1.936 GPa, respectively. Compared with the modulus (1.433 GPa) of cured DGEBA in Fig. 7a, the modulus of cured 12 wt% DSEHP-5/DGEBA blends increased by about (70.41%). The improvement in modulus may be attributed to the high tensile strength in Fig. 5a and high crosslink density. The crosslink density of DSEHP-n/DGEBA blends after curing can be obtained by the

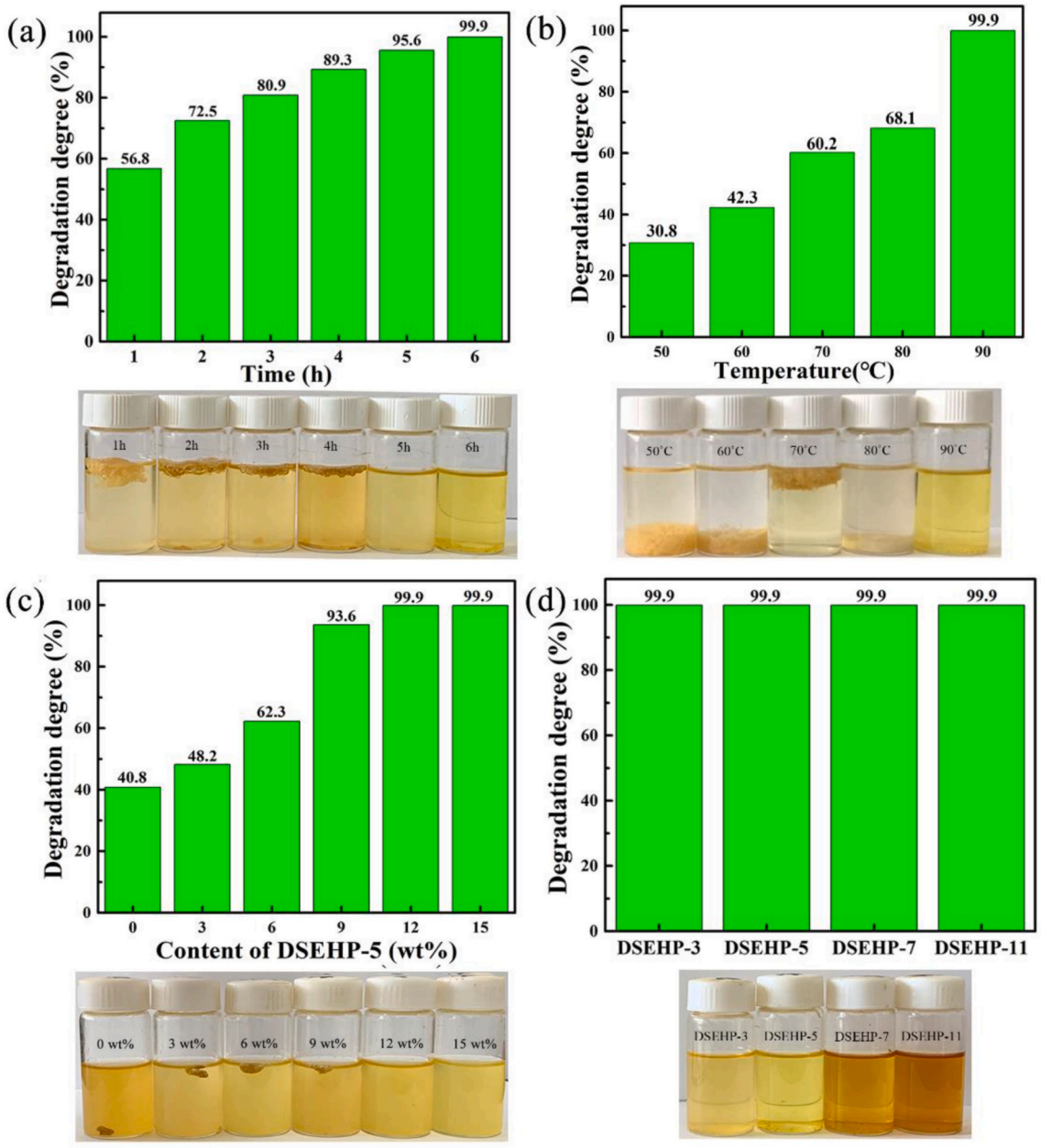


**Fig. 4.** The degradation behavior of DSEHP-n/DGEBA blends after curing (a. time, b. temperature, c. DSEHP-5 content, and d. molecular weight).

classical theory of rubber elasticity model [46,47] under the glass transition temperature ($T_g$) and the following equation (2).

$$\upsilon_e = \frac{E'}{3\varphi RT} \tag{2}$$

where $E'$ is the storage modulus at $T_g$+50 $K$, and $\varphi$ usually can be seen as 1, and the value R is 8.314 J•mol$^{-1}$/K. In the rubbery region ($T_g$+50 $K$), the storage modulus of 6 wt% DSEHP-5/DGEBA, 12 wt% DSEHP-5/DGEBA and 15 wt% DSEHP-5/DGEBA are 12.88 MPa, 16.34 MPa, 12.91 MPa, respectively. The crosslink density of the DSEHP-5/DGEBA blends raises firstly and then became lower along with the content of DSEHP-5 increasing in Fig. 7b. High crosslink density usually contributes to promoting the strength and modulus [48], resulting in high strength and high modulus of cured 12 wt% DSEHP-5/DGEBA blends.

$T_g$ was ascertained from the maximum of the tan $\delta$ or α-relaxation in Fig. 7c. It can be seen from Fig. 7c that appearance of the narrow single peaks for all the samples indicates the homogeneous structure and good compatibility [49] between DSEHP-5 and DGEBA. In the wake of the increase of DSEHP-5 content, the glass transition temperature of cured DSEHP-5/DGEBA composites decreases slightly, being attributable to the un-crosslinked structure in the core of DSEHP-5. In Fig. 7c, the β-relaxation peak temperatures of pure DGEBA, 6 wt% DSEHP-5/DGEBA, 12 wt% DSEHP-5/DGEBA, 15 wt% DSEHP-5/DGEBA are -9.43 °C, -15.06 °C, -25.89 °C, -29.67 °C, respectively. Compared with the pure DGEBA, the β-relaxation of the cured DSEHP-5/DGEBA blends shifts distinctly toward lower temperature and 12 wt% DSEHP-5/DGEBA decreased by 16.46 °C, which is often associated with the intermolecular hole or pendant group movements [36,50]. Our team had previously reported a low-temperature resistant epoxy resin [34]. Its β-relaxation peak temperature can reach about -40 °C, but its glass transition temperature is only about 85 °C, which limits the application of materials. Compared with it, the DSEHP-5/DGEBA blends have more superior comprehensive performance.

According to the free volume theory [51], the entire volume of a

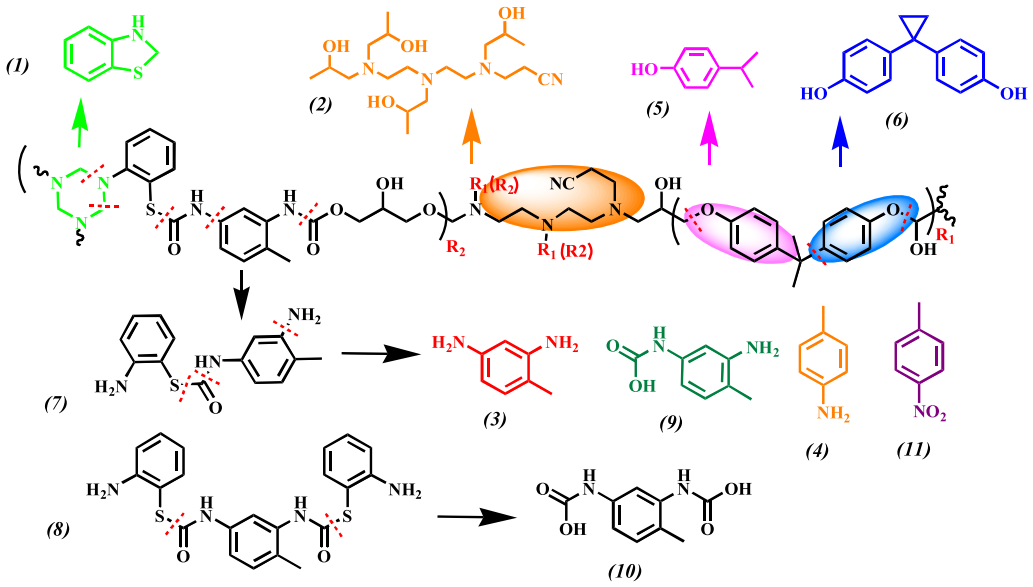


**Scheme 2.** Degradation mechanism of 12 wt% DSEHP-5/DGEBA blends after curing.

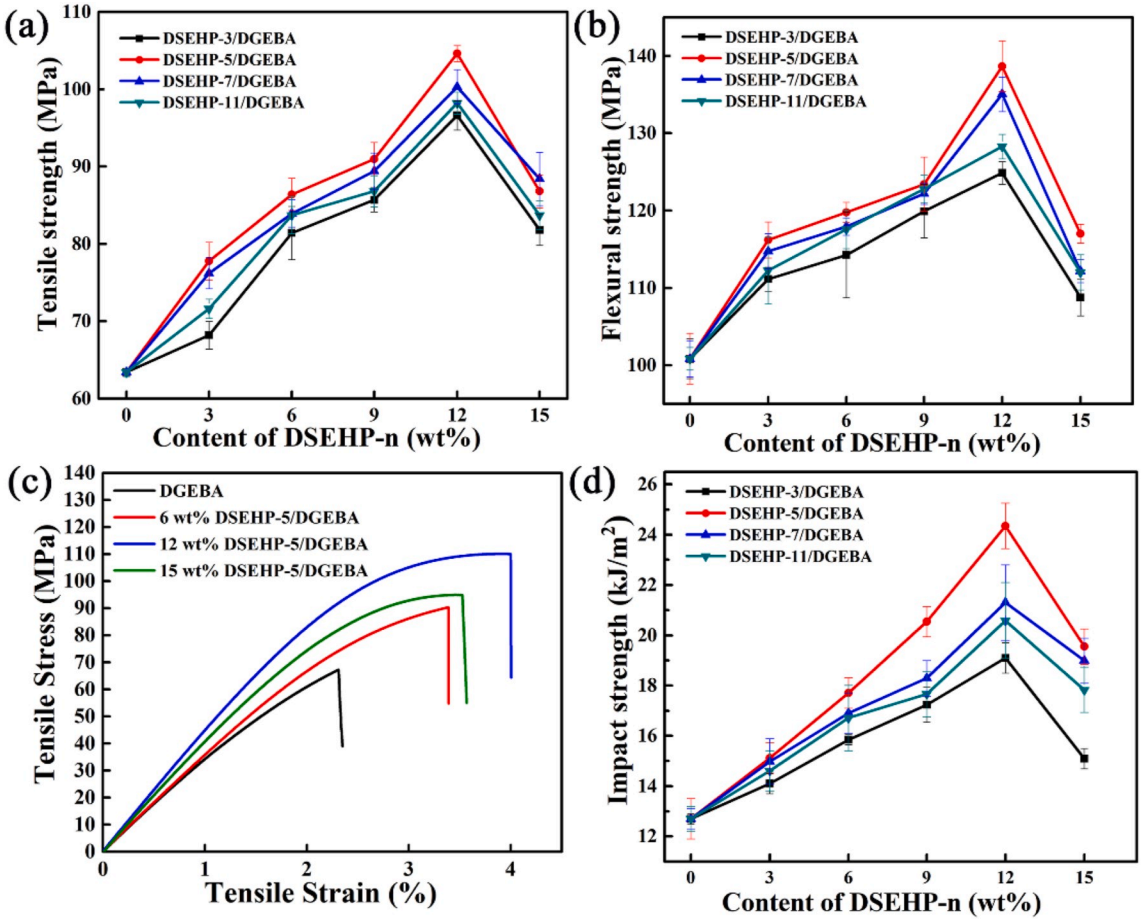


**Fig. 5.** The mechanical strengths of DSEHP-n/DGEBA blends after curing (a. tensile, b. flexural, c. strain or elongation, and d. impact).

liquid or solid includes two portions. A portion is the occupied volume which is occupied by the molecule itself, another portion is the free volume which is the space among the molecules. Occupied volume refers to the actual occupied volume of molecules or atoms in epoxy resin, while the free volume is randomly distributed in the polymer with the irregular size of holes, which provides a space for molecular activities, so that the molecular chain may adjust its conformation through rotation and displacement. The movement of the chain segment is frozen, and the free volume remains constant under the $T_g$. The size and distribution of the holes are basically fixed. With the increase of temperature, the

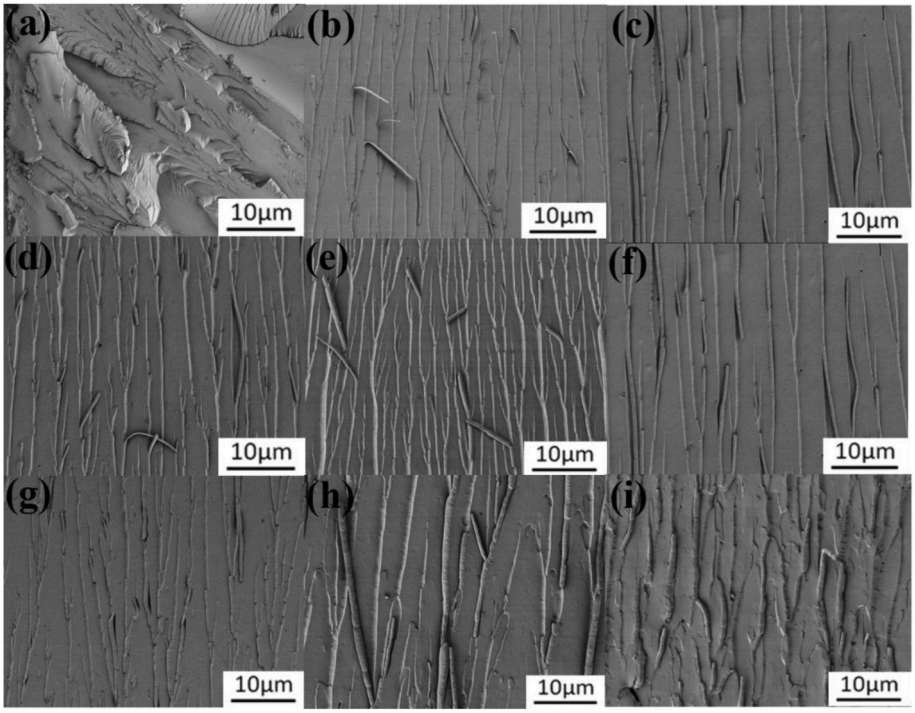


**Fig. 6.** SEM micrographs of impact fracture surface of blend materials (a. DGEBA, b. 3 wt% DSEHP-5/DGEBA, c. 6 wt% DSEHP-5/DGEBA, d. 9 wt% DSEHP-5/DGEBA, e. 12 wt% DSEHP-5/DGEBA, f. 15 wt% DSEHP-5/DGEBA, g. 12 wt% DSEHP-3/DGEBA, h. 12 wt% DSEHP-7/DGEBA, i. 12 wt% DSEHP-11/DGEBA).

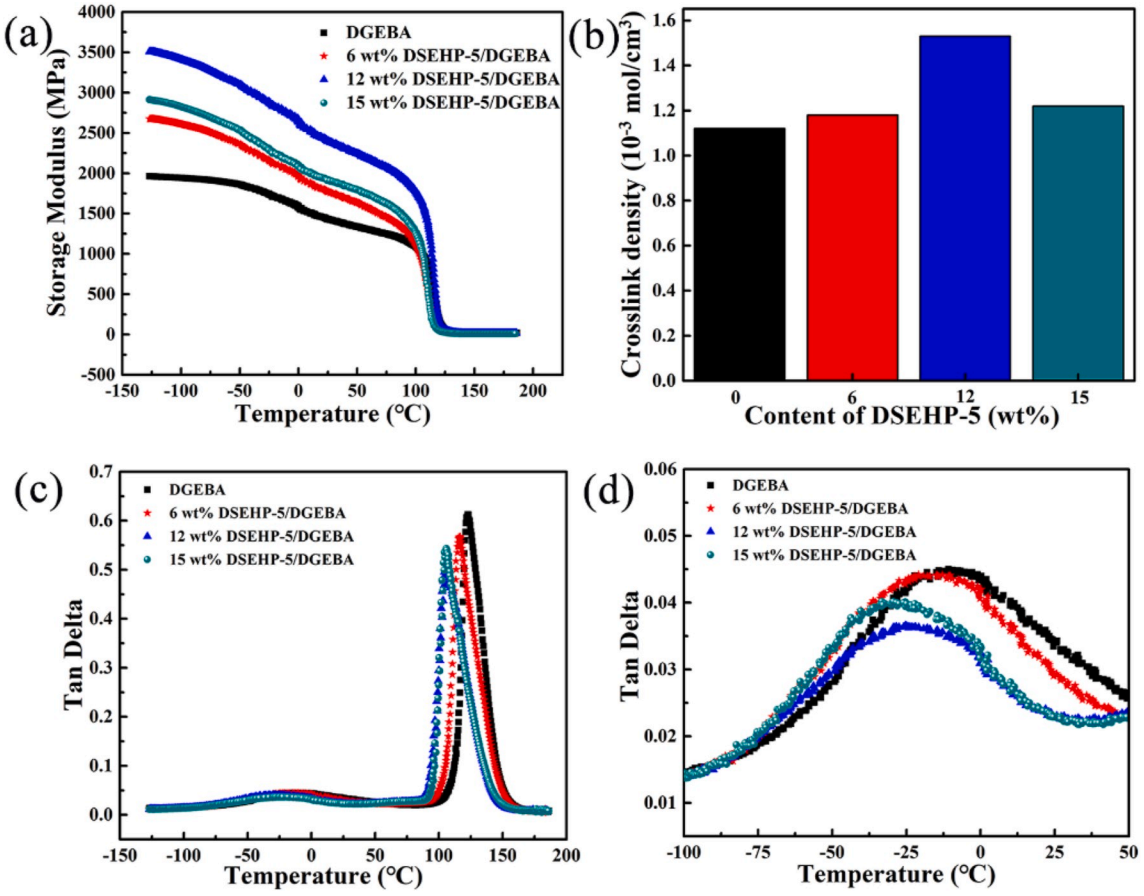


**Fig. 7.** Dynamic properties of DGEBA and DSEHP-5/DGEBA blends (a. storage modulus, b. crosslink density, c and d. tanδ).

expansion of resin volume is caused by the expansion of occupied volume. However, above the glass transition temperature, the chain segment motion is excited, the occupied volume and free volume will expand with the increase of temperature, so the volume expansion rate will be greater.

The DMA test with various frequencies shows that $T_g$ is a function of frequency in Table 1. As can see in Table 1, the $T_g$ raises with the increasing frequency, which can be explained by the Arrhenius equation. According to the Williams-Landel-Ferry (WLF) theory, Eq (3) is as follows:

$$\frac{1}{Log\frac{f}{f_r}} = \frac{C_2}{C_1}\left(\frac{1}{T_g - T_{gr}}\right) + \frac{1}{C_1} \tag{3}$$

where $f_r$ is the fixed frequency of 1 Hz, and $f$ is the frequency in DMA test, and both $C_1$ and $C_2$ are constants. But $C_1$ and $C_2$ also change with the addition of DSEHP-n, therefore, the $C_2/C_1$ is the slop: $\frac{1}{Log\frac{f}{f_r}} vs \frac{1}{T_g - T_{gr}}$

According to the free volume theory [51], Eq (4) and Eq (5) are as follows:

$$C_1 = \frac{B}{2.303 f_g},\ C_2 = \frac{f_g}{\triangle\alpha} \tag{4}$$

$$f_g = \left(\frac{\triangle\alpha \bullet B \bullet \frac{C_2}{C_1}}{2.303}\right)^{\frac{1}{2}} \tag{5}$$

where $B$ is a constant (about 1), and $f_g$ is the free volume fraction and α is the thermal expansion coefficient (CTE). $\triangle\alpha$ is the difference between the expansion coefficient between rubber state and glass state, which is $\alpha_r$-$\alpha_g$.

Table 2 shows the relationship between the coefficient of thermal expansion and the free volume fraction of blends. With the rise of DSEHP-5 content, the free volume and CTE ($\alpha_g$, $\alpha_r$) of cured DSEHP-n/DGEBA blends increased in the beginning and then became lower. The CTE of 12 wt% DSEHP-5/DGEBA blends is 78.23 × $10^{-6}$ $K^{-1}$, which is 18.59% lower than the 96.10 × $10^{-6}$ $K^{-1}$ of cured DGEBA at the same below the glass transition temperature. This has to do with the cross-linking density of the composite [52]. Above the glass transition temperature, the CTE of 12 wt% DSEHP-5/DGEBA blends is 187.90 × $10^{-6}$ $K^{-1}$, which is 5.96% higher than 176.70 × $10^{-6}$ $K^{-1}$ of DGEBA. This is mainly due to the increase of the intramolecular cavities in hyperbranched polymers and free volume fraction in cross-linked network structure [53]. There are a large number of rigid structures (benzene ring, triazine ring, etc.) and intramolecular cavity structures in DSEHP-n, so it will increase the free volume fraction of the material [54]. Below the glass transition temperature, the segments are frozen. As hyperbranched polymers are added, the crosslink density increases and the molecular motion is limited, resulting in decreases of the $\alpha_g$. Above the glass transition temperature, the frozen chain segment is unsealed and the free space is larger, so the $\alpha_r$ increases. In Table 2, the free volume fraction of the DSEHP-5/DGEBA was increased firstly and decreased secondly as the content of DSEHP-5 increasing. When the DSEHP-5 content was 12 wt%, both the thermal expansion coefficient and the free volume fraction of the composite reached the maximum value.

**Table 1**
Glass transition temperatures in different frequencies.

| Frequence (Hz) | DGEBA | 6 wt% DSEHP-5/DGEBA | 12 wt% DSEHP-5/DGEBA | 15 wt% DSEHP-5/DGEBA |
|---|---|---|---|---|
| 0.5 | 104.2 | 99.57 | 99.27 | 98.77 |
| 1 | 104.42 | 99.74 | 99.60 | 98.93 |
| 5 | 104.91 | 101.03 | 100.07 | 99.26 |
| 10 | 105.39 | 103.3 | 100.39 | 100.22 |
| 20 | 107.49 | 105.72 | 102.97 | 102 |
| 30 | 108.78 | 107.33 | 104.59 | 103.78 |
| 40 | 110.08 | 108.95 | 106.68 | 106.68 |
| 50 | 111.88 | 110.39 | 109.91 | 109.27 |

**Table 2**
CTE and $f_g$ of DGEBA and blends.

| Materials | $\alpha_g \times 10^{-6}$ ($K^{-1}$) | $\alpha_r \times 10^{-6}$ ($K^{-1}$) | $\triangle\alpha \times 10^{-6}$ ($K^{-1}$) | $f_g$ |
|---|---|---|---|---|
| DGEBA | 96.10 | 176.70 | 80.60 | 0.0052 |
| 6 wt% DSEHP-5/DGEBA | 79.16 | 181.50 | 102.35 | 0.0061 |
| 12 wt% DSEHP-5/DGEBA | 78.23 | 187.90 | 109.67 | 0.0082 |
| 15 wt% DSEHP-5/DGEBA | 88.08 | 191.20 | 103.12 | 0.0063 |

## 4. Conclusions

In summary, the influence of the DSEHP-n additive content and molecular mass on the properties of DSEHP-n/DGEBA blends after curing were discussed in detail. With the increase of DSEHP-n content, the viscosity and modulus of DSEHP-n/DGEBA blends increase, but the mechanical performances, free volume fraction and crosslinking density of the DSEHP-n/DGEBA blends increased firstly and decreased secondly. The maximum mechanical properties, modulus, and elongation achieved by 12 wt% DSEHP-5/DGEBA blends. SEM, DMA, and DLS demonstrated that there is no phase separation in the blends, and the improvement simultaneously on mechanical performance belongs to an in-situ reinforcing and toughening mechanism. It is important that DSEHP-5 could promote remarkably the degradation degree of DSEHP-5/DGEBA blends after curing about 2 times, and low-temperature resistance about 15 °C. The degradation mechanism was analyzed through GC-MS spectrogram and the formation of degradation products as a result of the cleavage of the C–N bond and ester bonds. This interesting result supplies an available method for preparing degradable thermoset composites with simultaneous high mechanical strength and low-temperature resistance.

## Declaration of competing interest

The authors declare that they have no known competing financial interests or personal relationships that could have appeared to influence the work reported in this paper.

## CRediT authorship contribution statement

**Xu Ma:** Methodology, Software, Data curation, Writing - original draft. **Wenqiang Guo:** Data curation, Writing - original draft. **Zejun Xu:** Writing - original draft. **Sufang Chen:** Data curation. **Juan Cheng:** Data curation. **Junheng Zhang:** Writing - review & editing. **Menghe Miao:** Writing - review & editing. **Daohong Zhang:** Supervision.

## Acknowledgments

We gratefully acknowledge financial support from the National Natural Science Foundation of China (51873233, 51573210 and 51703250), Hubei Provincial Natural Science Foundation (2018CFA023) and the Fundamental Research Funds for the Central Universities (CZP20006).

## Appendix A. Supplementary data

Supplementary data to this article can be found online at https://doi.org/10.1016/j.compositesb.2020.108005.

## References


[1] Fang F, Ran S, Fang Z, Song P, Wang H. Improved flame resistance and thermo-mechanical properties of epoxy resin nanocomposites from functionalized graphene oxide via self-assembly in water. Compos B Eng 2019;165:406–16.
[2] Jouyandeh M, Jazani OM, Navarchian AH, Shabanian M, Vahabi H, Saeb MR. Bushy-surface hybrid nanoparticles for developing epoxy superadhesives. Appl Surf Sci 2019;479:1148–60.
[3] Miao X, Xing A, Yang W, He L, Meng Y, Li X. Synthesis and characterization of hyperbranched polyether/DGEBA hybrid coatings. React Funct Polym 2018;122:116–22.
[4] Huo S, Yang S, Wang J, Cheng J, Zhang Q, Hu Y, et al. A liquid phosphorus-containing imidazole derivative as flame-retardant curing agent for epoxy resin with enhanced thermal latency, mechanical, and flame-retardant performances. J Hazard Mater 2020;386:121984.
[5] Fang F, Huo S, Shen H, Ran S, Wang H, Song P, et al. A bio-based ionic complex with different oxidation states of phosphorus for reducing flammability and smoke release of epoxy resins. Comput Commun 2020;17:104–8.
[6] Chen S, Xu Z, Zhang D. Synthesis and application of epoxy-ended hyperbranched polymers. Chem Eng J 2018;343:283–302.
[7] Garcia JM, Jones GO, Virwani K, McCloskey BD, Boday DJ, ter Huurne GM, et al. Recyclable, strong thermosets and organogels via paraformaldehyde condensation with diamines. Science 2014;344(6185):732–5.
[8] Montarnal D, Capelot M, Tournilhac F, Leibler L. Silica-like malleable materials from permanent organic networks. Science 2011;334:965–8.
[9] Ma S, Webster DC. Naturally occurring acids as cross-linkers to yield VOC-free, high-performance, fully bio-based, degradable thermosets. Macromolecules 2015;48(19):7127–37.
[10] Wang B, Ma S, Yan S. Readily recyclable carbon fiber reinforced composites based on degradable thermosets: a Review. Green Chem 2019:5781–96.
[11] Xu Z, Liang Y, Ma X, Chen S, Yu C, Wang Y, et al. Recyclable thermoset hyperbranched polymers containing reversible hexahydro-s-triazine. Nat Sustain 2020;3(1):29–34.
[12] Oliveux G, Dandy LO, Leeke GA. Current status of recycling of fibre reinforced polymers: review of technologies, reuse and resulting properties. Prog Mater Sci 2015;72:61–99.
[13] Yang P, Zhou Q, Yuan X-X, van Kasteren JMN, Wang Y-Z. Highly efficient solvolysis of epoxy resin using poly(ethylene glycol)/NaOH systems. Polym Degrad Stabil 2012;97(7):1101–6.
[14] Oh S, Choi D. Microbial community enhances biodegradation of bisphenol A through selection of sphingomonadaceae. Microb Ecol 2019;77(3):631–9.
[15] Liu Y, Kang H, Gong X, Jiang L, Liu Y, Wu S. Chemical decomposition of epoxy resin in near-critical water by an acid–base catalytic method. RSC Adv 2014;4(43):22367–73.
[16] Cheng H, Huang H, Liu Z, Zhang J. Reaction kinetics of CFRP degradation in supercritical fluids. J Polym Environ 2017;26(5):2153–65.
[17] Cicala G, Pergolizzi E, Piscopo F, Carbone D, Recca G. Hybrid composites manufactured by resin infusion with a fully recyclable bioepoxy resin. Compos B Eng 2018;132:69–76.
[18] Sarikaya E, Çallioğlu H, Demirel H. Production of epoxy composites reinforced by different natural fibers and their mechanical properties. Compos B Eng 2019;167:461–6.
[19] Yu C, Xu Z, Wang Y, Chen S, Miao M, Zhang D. Synthesis and degradation mechanism of self-cured hyperbranched epoxy resins from natural citric acid. ACS Omega 2018;3(7):8141–8.
[20] Ma S, Webster D. Hard and flexible, degradable thermosets from renewable bioresources with the assistance of water and ethanol. Macromolecules 2016;49:3780–8.
[21] Zhang ZP, Rong MZ, Zhang MQ. Polymer engineering based on reversible covalent chemistry: a promising innovative pathway towards new materials and new functionalities. Prog Polym Sci 2018;80:39–93.
[22] Johnson LM, Ledet E, Huffman ND, Swarner SL, Shepherd SD, Durham PG, et al. Controlled degradation of disulfide-based epoxy thermosets for extreme environments. Polymer 2015;64:84–92.
[23] Taynton P, Ni H, Zhu C, Yu K, Loob S, Jin Y, et al. Repairable woven carbon fiber composites with full recyclability enabled by malleable polyimine networks. Adv Mater 2016;28(15):2904–9.
[24] Guo W, Chen S, Cheng J, Zhang J, Miao M, Zhang D. Synthesis of renewable and self-curable thermosetting hyperbranched polymers by a click reaction. Prog Org Coating 2019;134:189–96.
[25] Ma Z, Wang Y, Zhu J, Yu J, Hu Z. Bio-based epoxy vitrimers: reprocessibility, controllable shape memory, and degradability. J Polym Sci, Polym Chem Ed 2017;55(10):1790–9.
[26] Lv C, Wang J, Li Z, Zhao K, Zheng J. Degradable, reprocessable, self-healing PDMS/CNTs nanocomposite elastomers with high stretchability and toughness based on novel dual-dynamic covalent sacrificial system. Compos B Eng 2019;177:107270.
[27] Yuan Y, Sun Y, Yan S, Zhao J, Liu S, Zhang M, et al. Multiply fully recyclable carbon fibre reinforced heat-resistant covalent thermosetting advanced composites. Nat Commun 2017;8:14657–66.
[28] Santos CM, Kumar A, Zhang W, Cai C. Functionalization of fluorous thin films via "click" chemistry. Chem Commun 2009;20:2854–6.
[29] Kaminker R, Callaway EB, Dolinski ND, Barbon SM, Shibata M, Wang H, et al. Solvent-free synthesis of high-performance polyhexahydrotriazine (PHT) thermosets. Chem Mater 2018;30(22):8352–8.
[30] You S, Ma S, Dai J, Jia Z, Liu X, Zhu J. Hexahydro-s-triazine: a trial for acid-degradable epoxy resins with high performance. ACS Sustainable Chem Eng 2017;5(6):4683–9.
[31] Dagdag O, Essamri A, El Gana L, El Bouchti M, Hamed O, Cherkaoui O, et al. Synthesis, characterization and rheological properties of epoxy monomers derived from bifunctional aromatic amines. Polym Bull 2018;76(9):4399–413.
[32] Yang S, Zhang Z, Wang F, Feng L, Jiang X, Yang C, et al. The synthesis and the bulk rheological properties of the highly-branched block polyethers. Polym Sci Ser A+ 2014;56(6):917–27.
[33] Roy B, Karak N. Modification of hyperbranched epoxy by vegetable oil-based highly branched polyester resin. Polym Bull 2012;68(9):2299–312.
[34] Wang Y, Chen S, Guo W, Miao M, Zhang D. The precise effect of degree of branching of epoxy-ended hyperbranched polymers on intrinsic property and performance. Prog Org Coating 2019;127:157–67.
[35] Hsissou R, Berradi M, El Bouchti M, El Bachiri A, El Harfi A. Synthesis characterization rheological and morphological study of a new epoxy resin pentaglycidyl ether pentaphenoxy of phosphorus and their composite (PGEPPP/MDA/PN). Polym Bull 2018;76(9):4859–78.
[36] Lu Y, Wang Y, Chen S, Zhang J, Cheng J, Miao M, Zhang D. Preparation of epoxy resins with excellent comprehensive performance by thiol-epoxy click reaction. Prog Org Coating 2020;139:105436.
[37] Yu Q, Liang Y, Cheng J, Chen S, Zhang A, Miao M, et al. Synthesis of a degradable high-performance epoxy-ended hyperbranched polyester. ACS Omega 2017;2(4):1350–9.
[38] Wang L, Chen S, Cheng J, Guo W, Wang Y, Miao M, et al. Synthesis of recyclable hyperbranched polymers with high efficiency of promoting degradation of epoxy resins. Chemistry 2018;3(17):4873–83.
[39] Xu P, Le C, Ding J. Chemical recycling of carbon fibre/epoxy composites in a mixed solution of peroxide hydrogen and N,N-dimethylformamide. Compos Sci Technol 2013;82:54–9.
[40] Yan H, Lu C-x, Jing D-q, Hou X-l. Chemical degradation of amine-cured DGEBA epoxy resin in supercritical 1-propanol for recycling carbon fiber from composites. Chin J Polym Sci 2014;32(11):1550–63.
[41] Rasschaert V, Goossens A. Conjunctivitis and bronchial asthma: symptoms of contact allergy to 1,3,5-tris (2-hydroxyethyl)-hexahydrotriazine (Grotan BK). Contact Dermatitis 2002;47:109–25.
[42] Wang Y, Chen S, Chen X, Lu Y, Miao M, Zhang D. Controllability of epoxy equivalent weight and performance of hyperbranched epoxy resins. Compos B Eng 2019;160:615–25.
[43] Duan Q, Wang S, Wang Q, Li T, Chen S, Miao M, et al. Simultaneous improvement on strength, modulus, and elongation of carbon nanotube films functionalized by hyperbranched polymers. ACS Appl Mater Interfaces 2019;11(39):36278–85.
[44] Wang X, Zong L, Han J, Wang J, Liu C, Jian X. Toughening and reinforcing of benzoxazine resins using a new hyperbranched polyether epoxy as a non-phase-separation modifier. Polymer 2017;121:217–27.
[45] Ricciardi MR, Papa I, Langella A, Langella T, Lopresto V. Mechanical properties of glass fibre composites based on nitrile rubber toughened modified epoxy resin. Compos B Eng 2018;139:259–67.
[46] Pistor V, Ornaghi FG, Ornaghi HL, Zattera AJ. Dynamic mechanical characterization of epoxy/epoxycyclohexyl–POSS nanocomposites. Mater Sci Eng, A 2012;532:339–45.
[47] Tang B, Kong M, Yang Q, Huang Y, Li G. Toward simultaneous toughening and reinforcing of trifunctional epoxies by low loading flexible reactive triblock copolymers. RSC Adv 2018;8(31):17380–8.
[48] Ricciardi MR, Papa I, Langella A, Langella T, Lopresto V, Antonucci V. Mechanical properties of glass fibre composites based on nitrile rubber toughened modified epoxy resin. Compos B Eng 2018;139:259–67.
[49] Zotti A, Zuppolini S, Borriello A, Zarrelli M. Thermal properties and fracture toughness of epoxy nanocomposites loaded with hyperbranched-polymers-based core/shell nanoparticles. Nanomaterials 2019;9(3):418.
[50] Yang S, Taha-Tijerina J, Serrato-Diaz V, Hernandez K, Lozano K. Dynamic mechanical and thermal analysis of aligned vapor grown carbon nanofiber reinforced polyethylene. Compos B Eng 2007;38:228–35.
[51] Montazeri A, Pourshamsian K, Riazian M. Viscoelastic properties and determination of free volume fraction of multi-walled carbon nanotube/epoxy composite using dynamic mechanical thermal analysis. Mater Des 2012;36:408–14.
[52] Luo L, Meng Y, Qiu T, Li X. An epoxy-ended hyperbranched polymer as a new modifier for toughening and reinforcing in epoxy resin. J Appl Polym Sci 2013;130(2):1064–73.
[53] Zhang J, Mi X, Chen S, Xu Z, Zhang D, Miao M, Wang J. A bio-based hyperbranched flame retardant for epoxy resins. Chem Eng J 2020;381:122719.
[54] Liu W, Zhou R, Sally L, Huang S, Lu X. From waste to functional additive: toughening epoxy resin with lignin. ACS Appl Mater Interfaces 2014;6(8):5810–7.